Seismically invisible water in Earth's transition zone?

Kirsten Schulze [a,*], Hauke Marquardt [a,b], Takaaki Kawazoe [c], Tiziana Boffa Ballaran [a], Catherine McCammon [a], Monika Koch-Müller [d], Alexander Kurnosov [a], Katharina Marquardt [a]

[a] *Bayerisches Geoinstitut BGI, University of Bayreuth, 95440 Bayreuth, Germany*
[b] *Department of Earth Sciences, University of Oxford, OX1 3AN Oxford, UK*
[c] *Department of Earth and Planetary Systems Sciences, Hiroshima University, 739-8526 Higashi-Hiroshima, Japan*
[d] *German Research Center for Geosciences GFZ, 14473 Potsdam, Germany*

ARTICLE INFO

ABSTRACT

Ringwoodite, the dominant mineral at depths between 520 km and 660 km, can store up to 2–3 wt.% of water in its crystal structure, making the Earth's transition zone a plausible water reservoir that plays a central role in Earth's deep water cycle. Experiments show that hydration of ringwoodite significantly reduces elastic wave velocities at room pressure, but the effect of pressure remains poorly constrained. Here, a novel experimental setup enables a direct quantification of the effect of hydration on ringwoodite single-crystal elasticity and density at pressures of the Earth's transition zone and high temperatures. Our data show that the hydration-induced reduction of seismic velocities almost vanishes at conditions of the transition zone. Seismic data thus agree with a wide range of water contents in the transition zone.

© 2018 Elsevier B.V. All rights reserved.

1. Introduction

The Earth's transition zone extends between depths of 410 km and 660 km and could host a water reservoir that has been stable over geological timescales, thereby playing a key role in the dynamic and geochemical evolution of the entire mantle (Bercovici and Karato, 2003). A hydrous transition zone might be associated with local melting events that are detectable above (Song et al., 2004) and below the transition zone (Schmandt et al., 2014) and may even be the source region for continental flood basalts (Wang et al., 2015), affecting the global climate and possibly contributing to mass extinction events throughout Earth's history.

The hypothesis of the transition zone being a deep water reservoir is based on high-pressure high-temperature experiments showing that the nominally anhydrous minerals $(Mg, Fe)_2SiO_4$ wadsleyite and ringwoodite, constituting up to 60 vol.% of transition zone rocks (Frost, 2008), can incorporate significant amounts of hydrogen ("water") as point defects into their crystal structures (Kohlstedt et al., 1996). The recent discovery of a hydrous ringwoodite inclusion in a natural diamond containing about 1.5 wt.% of water (Pearson et al., 2014) confirms experimental predictions and strengthens the hypothesis of a (at least partly) hydrated transition zone. However, this single observation does not constrain the global amount of water stored in the transition zone or its spatial distribution. Instead, global scale three-dimensional mapping of the water content in the transition zone requires geophysical remote sensing.

Previous experimental and theoretical studies have reported a significant reduction of elastic wave velocities with hydration for Mg_2SiO_4 ringwoodite (Inoue et al., 1998; Wang et al., 2003) as well as iron-bearing ringwoodite (Jacobsen et al., 2004) at ambient pressure. More limited experimental work indicates that this effect prevails to high pressures (Wang et al., 2006) and high temperatures (Mao et al., 2012), suggesting that reduced seismic wave velocities in the transition zone can be employed to map mantle hydration (Wang et al., 2006; Mao et al., 2012).

However, significant extrapolation of previous high-pressure experiments is required to quantify effects of hydration at transition zone pressures for ringwoodite, leading to contradictory conclusions (Fig. 1). In addition, the effect of temperature on the high-pressure elasticity of hydrous ringwoodite is mostly unconstrained. The only available measurement of the elastic wave velocities of hydrous iron-bearing ringwoodite at pressures up to 16 GPa and temperatures of up to 670 K suggests that tempera-

---

* Corresponding author.
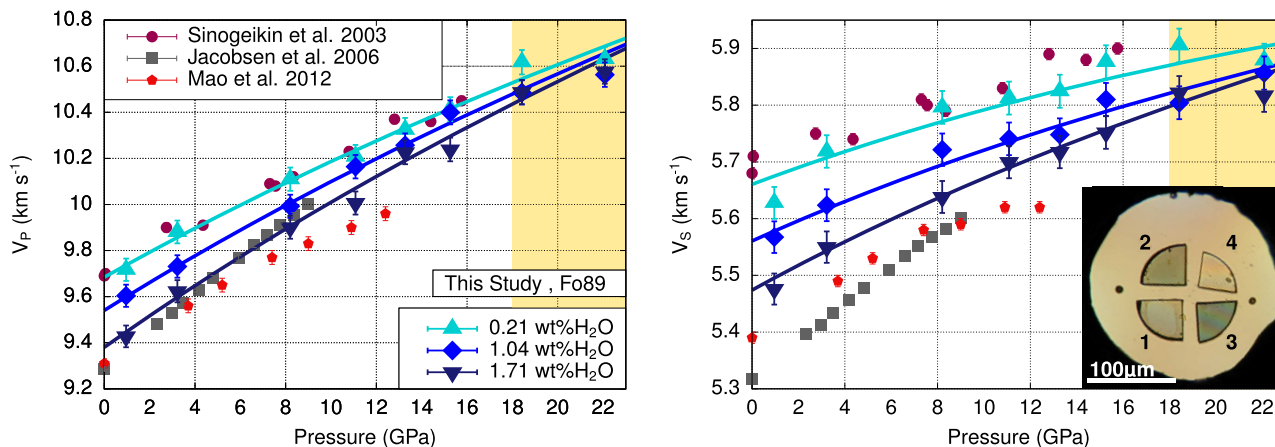*E-mail address:* Kirsten.Schulze@uni-bayreuth.de (K. Schulze).

Fig. 1. Measured high-pressure acoustic wave velocities of $(Mg_{0.89}Fe_{0.11})_2SiO_4$ ringwoodite in comparison to previously published work (Mao et al., 2012; Jacobsen and Smyth, 2006; Sinogeikin et al., 2003). The inset shows our experimental setup where we simultaneously measured three single-crystal samples of Fe-bearing ringwoodite and one Mg-ringwoodite to high pressures. Samples 1–3: Fe-bearing ringwoodites with 0.21(3), 1.04(11) and 1.71(18) wt.% H_2O. Sample 4: Mg_2SiO_4 ringwoodite with 0.42(5) wt.% H_2O (Table 4 in supplementary material).

ture may strongly enhance the hydration-induced velocity reduction for compressional wave velocities (Mao et al., 2012). However, the effects of a temperature increase to 670 K on the elastic wave velocities are comparably small (∼1–2% reduction), while uncertainties in pressure and temperature determination are large in resistively-heated diamond-anvil cell work. This combination results in significant uncertainties when comparing the results to high-pressure/-temperature experiments on anhydrous ringwoodite that suffer from the same uncertainties.

In order to reliably quantify the effect of hydration on the seismic wave velocities of ringwoodite at transition zone pressures and elevated temperatures, we designed a novel type of experiment, taking advantage of recent methodological developments (Marquardt and Marquardt, 2012; Kurnosov et al., 2017; Schulze et al., 2017). In our experiment, four focused ion beam (FIB) cut single-crystal samples of three hydrated $(Mg_{0.89}Fe_{0.11})_2SiO_4$ ringwoodite (Fo89) as well as one sample of Mg-ringwoodite (Fo100) were loaded together in the pressure chamber of a diamond-anvil cell (Fig. 1).

2. Material and methods

2.1. Sample synthesis and characterisation

San Carlos olivine was used as a starting material for synthesising the iron-containing ringwoodites. In two cases liquid water was added to synthesise hydrated samples. The Mg-endmember ringwoodite was grown from pure forsterite powder with no water added. The multi-anvil experimental conditions ranged between 19–22 GPa and 1200–1600 °C (Table 3 in supplementary material). The run products contained single crystals of ringwoodite with sizes on the order of 100 μm. For the iron-containing samples an increase in crystal size, structural quality and deepness of blue colour is observed with increasing water content. The Mg-endmember is colourless.

The hydration state of all samples was determined by unpolarized Fourier transform infrared spectroscopy (FTIR). FTIR was favoured over secondary ion mass spectroscopy (SIMS) as it allowed for measuring the hydration state of the double-side polished samples which were later loaded in the DAC. Depending on the platelet size, three to seven equally distributed FTIR spectra were taken for each platelet. All spectra were normalized and fringe (Neri et al., 1987) and background corrected. The integrated area and the position of the main peak between 2500 and 4000 cm^{-1} was calculated using a Voigt peak function. The

molar absorption coefficient was calculated from the calibration of Thomas et al. (2015) and the molar concentration using the Lambert–Beer law. All samples were measured on the same instrument and were processed identically. This procedure ensures a maximum degree of comparability among the samples. An uncertainty of 10% in derived water content is considered reasonable for all samples due to uncertainties in sample thickness, the peak-fitted integrated areas and the absorption coefficient (Thomas et al., 2015). For the conversion to the more commonly used unit of wt.% H_2O, the density at ambient conditions derived from the chemical analysis and x-ray diffraction was used. For the Fo89 composition water contents of 0.21(3) wt.%, 1.04(11) wt.% and 1.71(18) wt.% were determined for H4071, H4164 and H4166, respectively, as well as 0.42(5) wt.% for the Mg-endmember MA389.

To determine the oxidation state of the iron in the samples H4071, H4164 and H4166, both Mössbauer spectroscopy and electron energy loss spectroscopy (EELS) were performed at Bayerisches Geoinstitut (BGI) (Table 4, supplementary material). EELS was performed on the three iron-containing samples, but due to oxidation of the samples during measurement and despite considerable effort, only three evaluable spectra each could be acquired for H4071 and H4166. For all measurements high energy loss spectra and, for calibration, low energy loss spectra were acquired in a range of 670 to 772.35 eV and −10 to 92.35 eV, respectively. For each measurement an area on the sample was chosen manually and 50 frames were stacked to enhance spectrum quality, where the total exposure times were 250 s and 100 s for H4071 and H4166, respectively. The results for the ferric to total iron ratio $Fe^{3+}/\sum Fe$ range between 0.15 to 0.19 for H4071 and 0.10 to 0.15 for H4166.

Mössbauer spectroscopy was performed on samples extracted from high-pressure runs (either single crystal or polycrystalline aggregate) over regions of 500 μm diameter as previously described (McCammon et al., 2004). $Fe^{3+}/\sum Fe$ was determined from relative areas and uncertainties were assessed based on the results for different fitting models. The Mössbauer spectroscopy results are in good agreement with the results from EELS and are also in agreement with earlier studies (McCammon et al., 2004), considering both the absolute values and the absence of any correlation between hydration state and Fe^{3+} concentrations (Table 4 in supplementary material).

Electron microprobe analysis (EMPA) was performed on the three iron-bearing samples to determine the chemical composition. The Mg-endmember was synthesised from Mg_2SiO_4 and is